Laser and Particle Beams (2003), *21*, 123–138. Printed in the USA.

DOI: 10.1017/S0263034603212027

Current status of plasma emission electronics: I. Basic physical processes

V.I. GUSHENETS,[1] E.M. OKS,[1] G.YU. YUSHKOV,[1] AND N.G. REMPE[2]

[1]Institute of High Current Electronics, Siberian Division of the Russian Academy of Science, Tomsk, Russia
[2]State University of Control Systems and Radioelectronics, Tomsk, Russia

(Received 1 April 2003; Accepted 16 May 2003)

Abstract

This paper reviews the physical phenomena that accompany the emission of electrons and ions from plasma. The development of plasma emission electronics as an independent research field is closely associated with the name of its founder, Professor Kreindel Yu. E. The well-known advantages of plasma electron emitters (plasma cathodes) are the higher emission current density, the pulsed emission capability, and the wider range of residual gas pressures. A peculiar property of the plasma cathode is the possibility of extracting practically all electrons from plasma. The parameters of an ion and electron beam extracted from plasma carry information about the physical processes occurring in the plasma. This makes it possible to invoke emission methods to study the fundamental phenomena that take place in plasma of vacuum arc and low-pressures gas discharges.

Keywords: Arc discharge; Electron beam; Ion beam; Low-pressure gas discharge; Plasma; Time-of-light

1. INTRODUCTION

Since plasma consists of ions and electrons, its ability to emit these species is obvious and, hence, there is an opportunity to create plasma-system-based sources of charged particles with a broad spectrum of parameters for various applications. While the emission of ions from plasma seems to be the only way of producing ion beams (Brown, 1989; Wolf, 1995), the generation of electrons using systems with so-called plasma cathodes (Kreindel, 1977) can prove itself only if the plasma emitters of electrons show obvious advantages over many other means of generating electrons and, first of all, over hot cathodes. The well-known advantages of plasma electron sources are the higher emission current density, the pulsed emission capability, the wider range of residual gas pressures, the insensitivity to the residual gas, and others. Plasma cathodes appear to be especially advantageous in those cases where a hot cathode is not able to provide necessary parameters of the electron beam because of its limited emissive power or if it is operated under poor vacuum conditions. A peculiar property of plasma cathodes is the possibility of extraction of practically all electrons from the plasma. This property is responsible for the high efficiency of this type of electron emitter. On the other hand, the experience gained in developing highly efficient plasma cathodes can be used in creating plasma sources of ions. It should also be noted that the parameters of an ion or electron beam extracted from a plasma carry information about the main physical processes occurring in the plasma. This makes it possible to invoke emission methods to study the fundamental phenomena that take place in plasmas and low-pressure gas discharges.

The development of plasma emission electronics as an independent research field is closely associated with the name of its founder, Professor Yuly E. Kreindel (Kreindel, 1977; Zavialov *et al.*, 1988). He supervised the pioneering studies on the emission of charged particles from discharge plasmas at Tomsk Institute of Control Systems and Radioelectronics (now Tomsk State University of Control Systems and Radioelectronics—TSUCSR). This line of research was given powerful impetus when the laboratory of plasma emission electronics headed by Yu. E. Kreindel was organized at the Institute of High Current Electronics (IHCE) of the Russian Academy of Sciences, established by Academician Gennady A. Mesyats in 1977. A substantial contribution to the development of plasma emission electronics was made by professors A.V. Zharinov (Zarinov *et al.*, 1986), P.M. Schanin (Bugaev *et al.*, 1980), V.A. Gruzdev (Galansky *et al.*, 1990), and many others (Gruzdev & Rempe, 1982; Koval *et al.*, 1992; Hershcovitch *et al.*, 1998; Oks & Schanin, 1999; Gavrilov & Oks, 2000; Goebel & Watkings, 2000).

Address correspondence and reprint requests to: Efim Oks, High Current Electronics Institute, 4 Akademichesky Ave., 634055 Tomsk, Russia. E-mail: oks@opee.hcei.tsc.ru

This article and a companion article (Bugaev *et al.*, this issue) review the studies in this field performed in recent years in the IHCE and in the laboratory of plasma electronics (TSUCSR). In this first article, attention is focused on the physical phenomena that accompany the emission of ions and electrons from plasma. The second part presents recent versions of the plasma sources of electrons and ions developed based on the studies of the emissive properties of plasmas and gives some examples of their practical use.

2. PHYSICAL FOUNDATIONS OF THE EMISSION OF CHARGED PARTICLES FROM PLASMA

When considered in general, the processes of emission of ions and electrons from plasma should be identical. The same phenomena are inherent in both processes. However, in a specific plasma-generating gas-discharge system, the conditions for the current passage and current closing to the electrodes are different for ions and electrons: while ions, as a rule, are accelerated in the near-electrode layer, electrons are decelerated in this layer. Therefore, when extracting charged particles from a plasma, one should expect that the ion-emission capabilities of the plasma are substantially different from the properties the plasma shows in the case of extraction of electrons.

2.1. Emission of ions

We shall restrict our consideration to the case that is most frequently met in charged particle sources, namely, when the plasma, due to the higher mobility of electrons, is charged positively with respect to the walls and electrodes of the discharge chamber. For definiteness, we assume that ions are extracted from the near-anode plasma toward a collector of area S_e (Fig. 1). The collector is at a potential difference U_a relative to the anode, which accelerates the ions. When the collector and anode potentials are equal ($U_a = 0$), the collector is a part of the discharge chamber anode, and a positive space charge layer, which decelerates electrons and accelerates ions, similar to the near-anode layer, is formed at the collector. The collector current density j_i is determined by the well-known Bohm relation

$$j_i = 0.4en_0(2kT_e/M)^{1/2}. \tag{1}$$

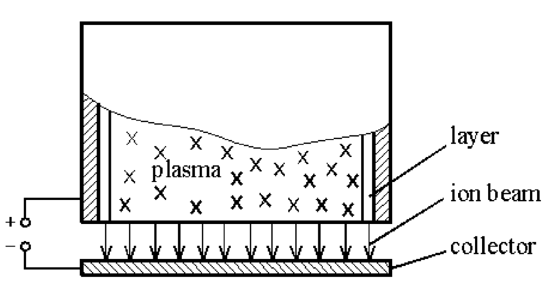

Fig. 1. Sketch of the ion diode.

Here, n_0 is the plasma density, T_e is the plasma electron temperature, M_i is the ion mass, e is the electron charge, and k is Boltzmann's constant.

If the plasma parameters are uniformly distributed throughout the volume, it can be stated that the total ion current is distributed between the anode and the collector proportional to their areas. As a negative bias is applied to the collector relative to the anode, the plasma will react to the external electric field, and the opening space charge layer will screen it from this field. The greater the potential difference between the collector and the anode, the farther the plasma is away from the collector and the broader is the ion layer. In this case, the ion current density is determined by the plasma density and electron temperature and the ion energy depends on the choice of the collector potential relative to the anode. It should be noted that the total energy of accelerated electrons E_i is then given by

$$\begin{aligned} E_i &= kT_e/2 - e(\varphi_a - \varphi_p) - e(\varphi_c - \varphi_a) \\ &= kT_e/2 - e(\varphi_c - \varphi_p). \end{aligned} \tag{2}$$

Here, φ_a, φ_p, and φ_c are the anode, plasma, and collector potentials, respectively (for the case of ions extracted from plasma, we have $\varphi_p > \varphi_a > \varphi_c$).

Thus, one of the most important features of a plasma ion diode is a mobile plasma boundary with the density of the ion current extracted from the plasma remaining unchanged. The density of an ion current extracted from plasma is in any case the saturation current density, that is, the maximum value that can be provided by the plasma, proceeding from the realized parameters. The electric field at a plasma boundary is always equal to zero. Since, in general, ions are accelerated by a voltage U_a of tens of kilovolts, which is much greater than the electron temperature, it can be considered that in plasma ion sources, the plasma electrons are in fact reflected from the layer boundary. This makes the layer purely ionic and this in turn allows one to determine rather accurately its width l_i by equating the Child–Langmuir and Bohm relations:

$$(4/9)(2e/M_i)^{1/2}\varepsilon_0 U_a^{3/2}/l_i^2 = 0.4en_0(2kT_e/M_i)^{1/2}. \tag{3}$$

Ions are generally extracted from the plasma through one or several holes in the anode of the discharge chamber. Depending on the relation between the plasma density and electron temperature, on the one hand, and the external electric field that accelerates the ions, on the other hand, three different positions of the established plasma boundary are possible (Fig. 2):

1. A high-density plasma and/or a weak field. In this case, the width of the ion layer is small, the plasma comes out from the anode hole, and the plasma boundary is formed in the acceleration gap (Fig. 2a). This, as

https://doi.org/10.1017/S0263034603212027 Published online by Cambridge University Press

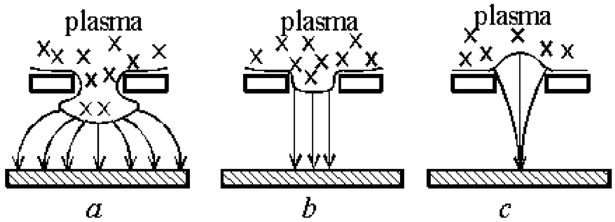

Fig. 2. Three possible conditions of the extraction of ions from plasma.

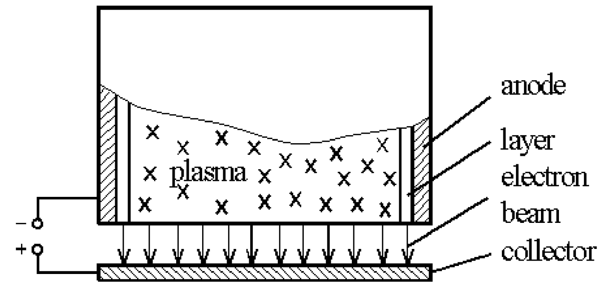

Fig. 3. Sketch of the plasma cathode.

can be seen in Figure 2a, results in defocusing of the ion beam.

2. The plasma and accelerating field parameters are optimum for a given geometry. With reference to case (1), the optimum conditions are attained by increasing electric field or by decreasing plasma density. As this takes place, the plasma boundary shifts toward the anode hole and is fixed in the plane of the latter, and this provides for the formation of a plane-parallel ion beam (Fig. 2b).
3. A low-density plasma and/or a strong field. Further increasing accelerating field or decreasing charged particle density in the plasma move it to behind the emission hole in the anode. The accelerating field penetrates into the anode region, and the plasma boundary is settled behind the anode hole (Fig. 2c). This results in focusing of the ion beam.

When ions are extracted from a plasma charged positively with respect to the emission electrode, the accelerating field of the collector coincides with the field of the layer, and this provides merely additional acceleration of ions. The density of the ion current emitted by the plasma is Bohm's density, and it coincides with the density of the current onto the anode and other electrodes of the discharge chamber to which ions may go. Therefore, if the plasma parameters are distributed uniformly, the ions borne in the plasma are spread among the discharge chamber electrodes and the collector proportional to their areas. However, the same situation takes place in the original state when the potential difference between the collector and the anode is equal to zero. This allows the conclusion that the in most frequent case of a negative fall potential near the emission electrode, the emission of ions from the plasma causes no change in its parameters and, hence, does not disturb the plasma.

2.2. Emission of electrons

By the term a "plasma emitter of electrons," or "plasma cathode," is meant an electric-discharge device which produces a plasma from the boundary of which electron emission occurs. The simplest schematic diagram of a plasma cathode is shown in Figure 3.

The device includes a plasma generator, the plasma emission surface, and an accelerating electrode collector, which is at a voltage with respect to one of the discharge system electrodes (cathode or anode) that accelerates electrons. For definiteness, we shall consider the anode electrode the reference electrode (with reference to which the accelerating potential difference is applied). For the majority of cases, the anode fall potential is negative, and electrons, in contrast to ions, arrive at the anode having overcome a potential barrier. It is the different conditions under which ions and electrons go away from plasma that are responsible for the difference between the emission of electrons from plasma and the emission of ions. In general, for charged particles to be accelerated by an external field, it is necessary that an increase in applied voltage lead to a corresponding increase in particle velocity. When ions are extracted from a positively charged plasma, this criterion is fulfilled in a natural way since the ions are only additionally accelerated by the applied electric field. The situation is radically different if electrons are emitted by such a plasma. If the potential difference between the anode and the collector is equal to zero, the latter, as with the extraction of ions, is a part of the anode. In this case, the electrons arrive at the anode having overcome a potential barrier, which is no different from the near-anode barrier. It follows that for the potential difference zero, the density of the electron current onto the collector coincides with the density of the electron current onto the anode. It should also be noted that the electrons are decelerated, not accelerated, as happens with ions. Therefore, if an electron-accelerating potential is applied to the collector earlier than the particles start to be accelerated, the potential barrier for electrons becomes lower due to the imposition of the accelerating field on the field of the near-electrode layer. Since the density of an electron current through a barrier, j_e, is determined by the Boltzmann relation

$$j_e = j_{ex} \exp[-e(\varphi_p - \varphi_c)], \tag{4}$$

where $j_{ex} = en_e\nu_e/4$ is the density of the chaotic electron current from plasma, the lowering of the barrier increases the density of the electron current onto the collector. When the generation of charged particles in plasma is balanced by their losses, this increase in current density is possible only in the case in which the current is redistributed between the anode and the collector. Since the anode current density j_a can be determined as

https://doi.org/10.1017/S0263034603212027 Published online by Cambridge University Press

$$j_a = j_{ex}\exp[-e(\varphi_p - \varphi_a)], \quad (5)$$

the most probable way of decreasing anode current density is associated with an increase in plasma potential and a corresponding heightening of the potential barrier for the electrons going away toward the anode.

Thus, attempts to accelerate electrons coming out from the plasma toward the collector lead to an increase in plasma potential, and this, according to (4), compensates the lowering of the potential barrier for these electrons. The plasma reacts to this increase of its potential. Obviously, the acceleration of electrons is possible if, as the accelerating voltage applied between the collector and the anode is increased, the collector potential reaches the plasma potential, despite the corresponding increase in plasma potential, and then even exceeds the latter by the required energy of the accelerated electrons. It should be noted that as this takes place, the density of the electron current from the plasma reaches its maximum value (saturation current density) equal to j_{ex}.

Since in (4) φ_p depends on φ_c, this relation is indefinite and cannot be considered the emission relation for a plasma cathode. Additionally, it is necessary to reveal the relation between the emission and discharge parameters that should be determined by the type of discharge used and by the discharge gap geometry. However, it is possible to distinguish some properties of plasma cathodes common in all types of discharge by which they operate. Zharinov (unpubl.), having analyzed the phenomena involved in the emission of electrons from plasma, has established a relation that can be considered a criterion for occurrence of acceleration of electrons extracted from plasma:

$$GS_e/(S_e + S_a) \leq 1. \quad (6)$$

Here, S_e is the area of the plasma emission surface, S_a is the area of the anode surface (in general, the net area of the surfaces of all electrodes to which electrons can go away from the discharge gap), and G is a parameter of the discharge, which is approximately equal to the ratio of the chaotic electron current density to the density of the electron current onto the anode for no extraction of electrons from the plasma. For discharges with a negative anode fall potential, we have $G \geq 1$.

Criterion (6) is in fact a corollary from the condition of continuity of the discharge current. This criterion implies that if the barrier is eliminated, the maximum electron emission current is not over the discharge current. Obviously, under steady-state conditions, the number of electrons that can be extracted from plasma is restricted by the rate of their generation. If this condition is not fulfilled, the collector current will reach the discharge current earlier than the collector potential will reach the plasma potential. Since further increase in collector current is impossible, an increase in collector potential will then be accompanied by a respective increase in plasma potential, so that $\varphi_p \geq \varphi_c$ will always be true, that is, the collector potential will remain lower than the plasma potential and the acceleration of electrons will be impossible. Thus, the limiting condition for the feasibility of the extraction and acceleration of plasma electrons is that the collector potential reaches the plasma potential with the collector current equal to the discharge current. It should be noted that, in contrast to the extraction of ions, the emission and anode current are not distributed proportionally to the areas S_e and S_a. As follows from (6), owing to the rather great value of the discharge parameter G (this implies that the chaotic current density in the plasma is much greater than the density of the electron current onto the anode), the collector current can be almost equal to the discharge current if the area of the plasma emission surface is relatively small. This is the so-called effect of current switching in a plasma cathode, which is widely used in developing plasma-cathode electron sources. The opportunity of current switching is also a distinguishing feature of the electron emission from plasma compared to the ion emission.

If the criterion for the acceleration of electrons extracted from the plasma is fulfilled, the behavior of the plasma boundary on varying accelerating field is practically the same as in the case of extraction of ions. The width of the negative space charge layer across which the electron-accelerating voltage falls is determined by a relation similar to (3):

$$(4/9)(2e/m_e)^{1/2}\varepsilon_0 U_a^{3/2}/l_e^2 = en_0(kT_e/2\pi m_e)^{1/2}. \quad (7)$$

For the extraction of electrons from a plasma, depending on the relation between the plasma parameters and the electric field, as for the emission of ions, three characteristic configurations of the established plasma boundary are possible that result in defocusing of the ion beam, in the formation of a plane-parallel beam, or in focusing of the beam.

Experiments have shown that the effect of the electron emission on the plasma parameters is not limited to variations in the plasma potential. The extraction of electrons from a plasma may also be accompanied by variations in plasma density, an increase or decrease in discharge current, and appearance of high-frequency oscillations; in some cases, electron emission made the discharge unstable and even caused its extinction. Therefore, the emission of electrons from an unclosed plasma surface, despite the fact that it offers the possibility to attain high emissive parameters, has not found application. In actual plasma-cathode electron sources, the plasma emission surface has limited dimensions which are comparable to the width of the space charge layer that appears near the electrode that has one or several emission holes. A method of realization of this principle is to cover the plasma emission surface with a fine metal grid whose mesh size is comparable to the width of the near-electrode layer. Therefore, this method is called the "grid (layer) stabilization method."

The principle of grid stabilization is as follows: The width of the space charge layer that separates the plasma from the electrode can be estimated for the most frequent case of a negative anode fall potential from the equality of the anode ion current density values determined by the Bohm relation and the Child–Langmuir law for ion current:

$$l_l = (\varepsilon_0/n)^{1/2}(\varphi_p - \varphi_a)^{3/4}/(ekT_e)^{1/4}. \tag{8}$$

When the size of the emission hole (grid mesh) is of the order of the layer width, the electron emission from the plasma occurs from a partially open surface: At the center, it takes place from an open surface due to the fact that the layers do not superimpose, while at the edges, the emitted electrons pass through a potential barrier. In this case, the open plasma surface contracts with increasing layer width. Since the emission current density in the absence of a barrier is much greater than the density of the current of electrons overcoming a barrier, the total emission current from plasma is determined in the main by the area of the plasma open surface.

Let us consider the grid stabilization mechanism. Assume that in the course of the extraction of electrons from plasma the electron emission current has increased due to a fluctuation. This will result in an increase in plasma potential relative to the anode and, as a consequence, according to (8), to a widening of the near-anode layer. Due to the wider layer in the hole, the area of the open plasma surface will decrease, resulting in a decrease in electron emission current. Thus, there exists a negative feedback between the layer and emission parameters, which ensures stabilization of the electron emission current.

In general, depending on the proportion between the size of the emission hole (grid mesh) h and the layer width l_l, three various mechanisms for the emission of electrons from plasma are possible:

1. If the emission hole is smaller than the layer in width ($h \ll l_l$), the layers completely close the emission hole and the electron emission occurs through a potential barrier. In the limiting case, this barrier coincides in height with the potential barrier for the electrons going away toward the anode. Therefore, the emission current density coincides with the anode current density. It can readily be shown that in this case, the efficiency of electron extraction α (emission-to-discharge current ratio) with an anode area S_a is given by

$$\alpha = S_e/(S_e + S_a). \tag{9}$$

Since, for this case, the emission and anode current densities are equal and there is no redistribution of the electron current between the collector and the anode on application of an accelerating potential, the electron emission does not disturb the discharge. However, because of the small size of the emission hole, the efficiency of electron extraction is not over several percent.

2. Another limiting case is the situation where $h \gg l_l$. In this case, the space charge layer is so narrow compared to the emission hole that the open plasma surface occupies the whole of the emission surface. The emission current density is equal to the density of the chaotic current from the plasma, which is substantially greater than the anode current density. For this case, we have

$$\alpha = S_e/(S_e + S_a)\exp[e(\varphi_p - \varphi_a)]. \tag{10}$$

The efficiency of electron extraction approaches its maximum value equal to unity. However, the degree of disturbance of the plasma parameters may appear rather high, presenting a challenge with producing an electron beam with stable parameters.

For these two cases, the grid stabilization effect does not show up, since the width of the space charge layer is either much greater or much less than the characteristic size of the emission surface. The most practicable case is one intermediate between cases (1) and (2).

3. In this case, $h \approx l_l$, and we have $\alpha \approx 0.5$. With this rather high efficiency of electron extraction, the grid stabilization of the plasma parameters shows up in full measure and the variations in plasma parameters that accompany the process of electron emission are not pronounced.

Thus, with a negative near-electrode fall potential, the ion emission from the plasma does not disturb the discharge, while the electron emission results in substantial changes in parameters of both the plasma and the discharge parameters, preventing efficient extraction and acceleration of electrons. Thus, there are more differences of principle rather than similarities in the processes of emission of ions and electrons from plasma. It should be noted, however, that strictly reverse conditions can be created for ions and electrons going away from plasma. For instance, in a weak transverse magnetic field, the mobility of electrons is lower than that of yet nonmagnetized ions, and the plasma is charged negatively to confine the ions, the faster species. The positive anode fall that appeared will accelerate electrons and decelerate ions, resulting in the inversion of the emissive properties of the plasma with respect to ions and electrons. In this situation, the electron emission current will be strictly proportional to the ratio of the area of the emission surface to the anode area and the extraction of electrons will not disturb the plasma. However, for the emission of ions, all mentioned features of the electron emission—from the variation of the plasma potential to the effect of switching of the current onto the collector—will show up. This is unambiguously evidenced by our experiments on the extraction of ions from the plasma of an arc discharge (Zharinov, 1980).

It should be noted that the above mechanisms for the emission of charged particles from plasma are based on very simplified models of emitters and give only general notions about the plasma and emission processes occurring in gas-discharge systems. For actual plasma-emitter sources of charged particles, when analyzing their emissive properties, it is necessary to take into account many factors such as the mode of discharge operation, the distributions of the plasma parameters, the shape and geometric dimensions of the electrodes of the discharge chamber, the variations in plasma properties in the emission channel (channels), and so forth. In this case, one cannot consider the factors that affect the emissive properties of electron emitters without considering the whole combination of the interrelated processes of generation and loss of charged particles in the gas discharge, and in the emission region, taking account of the influence of the near-electrode layers on the emission parameters. This approach is also of interest in that it allows one to reveal additional emission processes and mechanisms for the influence of the emission of charged particles from plasma on the properties of the gas discharge, which are not considered in terms of generalized models. By way of example, let us consider in more detail the plasma and emission processes in electron emitters based on a reflected discharge.

2.3. Plasma and emission processes in reflected-discharge-based electron emitters

The electron sources in which the emitting plasma is generated in a reflected discharge in a magnetic field with the use of the so-called hollow-cathode effect for increasing plasma density have found practical implementation (Kreindel, 1983). In this type of discharge, plasma is generated in the intercathode space and in the hollow cathode. In the intercathode space, a nonequilibrium charged particle density distribution is established due to the interaction of two plasma regions with different conditions for the motion of charged particles. The plasma density in the near-axis region of the intercathode space is greater than the plasma density near the hole of the cathode cavity. With that, the axial distribution of the plasma potential in the discharge is such that the cavity is a source of electrons. The motion of the electrons supplied by the hollow cathode into the electrode gap is limited by the transverse magnetic field. These electrons are accumulated in the near-axis discharge region and vary the plasma potential and density until conditions (corresponding density and potential gradients) for their transfer to the anode are created. Eventually, in this type of discharge, the plasma potential appears to be substantially (by 15–20%) lower than the anode potential (discharge with a positive anode fall voltage). Ionization of the gas in the intercathode space is effected predominantly by fast electrons that are borne due to γ-processes at flat parts of the hollow and emitter cathodes and oscillate in the intercathode space. If the fall potential at the exit of the cavity is higher than the ionization potential of the working gas, ionization by the electrons of the cavity is also possible. For this pattern, the parameters of the plasma in the intercathode space of the discharge can be calculated by solving jointly the continuity equations and the equations of motion for electrons and ions. We consider only the simplest case where charged particles are transferred to the anode across a magnetic field by "classical" mechanisms. Then the system of equations that describe the plasma can be represented in the form (Schanin, 1993)

$$\frac{dj_{er}}{dr} + \frac{j_{er}}{r} = (\beta + \gamma\chi)n_i(r) + \xi + \lambda, \tag{11}$$

$$\frac{dj_{ir}}{dr} + \frac{j_{ir}}{r} = (\beta - \chi)n_i(r) + \xi, \tag{12}$$

$$j_{er} = D_{e\perp}\frac{dn_e(r)}{dr} + \mu_{e\perp}n_e(r)\frac{d\varphi(r)}{dr}, \tag{13}$$

$$j_{ir} = -D_{i\perp}\frac{dn_i(r)}{dr} - \mu_{i\perp}n_i(r)\frac{d\varphi(r)}{dr}, \tag{14}$$

where j is the particle flow density; $D_\perp$ and $\mu_\perp$ are, respectively, the coefficients of diffusion and mobility across the magnetic field; $n(r)$ and $\varphi(r)$ are the plasma density and potential, respectively; β is the number of ionizing acts executed by a γ-electron; ξ is the number of ionizing acts executed by an electron that came out of the cavity; $\chi = 0.4(2kT_e/M_i)^{1/2}L^{-1}$ and $\lambda = mI_p/(e\pi r_0^2 L)$ are the number of electrons coming from the cavity into a unit volume of the intercathode space in a unit time.

Equations (11)–(14) combined with the quasi-neutrality condition $n_i(r) = n_e(r)$ form a system of equations which allows one to calculate the radial distributions of the plasma parameters. As follows from calculations, the plasma density peaks in the near-axis region of a discharge. It follows that to attain a high density of the emission current, it is appropriate to extract electrons from the near-axis region of the discharge through a channel or a system of channels made in the cathode.

The emission channel in an electron emitter fulfills different functions. In particular, the channel separates the plasma production and the beam acceleration regions, limiting the penetration of the field of the acceleration electrodes into the discharge chamber and creating a required pressure difference between the discharge chamber and the acceleration gap. In this connection, there exist some limiting geometric dimensions of the channel at which stable operation of the electron source is ensured. At the same time, a decrease in the diameter of the hole or an increase in the length of the channel for the same discharge current results in a decrease in emission current, which cannot be explained only by the respective decrease in emission area. It can be suggested that the emission channel has some effect on the parameters of the plasma that penetrate into the channel. Experiments have shown that the penetration of the plasma into the emission channel is accompanied by a decrease in its density and the appearance of an axial electric field, which returns the electrons into the discharge gap. The decrease in plasma density leads to the growth of the near-wall space charge layer, and this eventually may limit the plasma penetration depth.

The parameters of the plasma in the channel can be found by solving the continuity equation (Schanin, 1993)

$$\frac{dN_z}{dz}(U_0 - U_z + 0.5) + N_z\rho_z\left[(U_0 - U_z)^{1/2}\frac{0.8}{R} - 2\,\frac{U_0 - U_z}{\rho_z}\frac{d\rho_z}{dz}\right] = 0, \quad (15)$$

where $N_z = n(z)/n_0$, $\rho_z = r/r_z$, $U_z = e\varphi(z)/kT_e$, $U_0 = e\varphi_0/kT_e$, n_0 *and* φ_0 are the plasma density and potential at the inlet of the channel of radius r, and r_z is the radius of the plasma at the distance z from the channel exit.

Since the electrons are in a longitudinal brake field and are considered thermodynamically at equilibrium, we can assume that they obey the Boltzmann axial density distribution

$$N_z = \exp(U_z - U_0). \quad (16)$$

The calculated axial distributions of the plasma density and potential (Fig. 4) are in satisfactory agreement with experimental data.

Analysis of the numerical simulation results has shown that for given values of n_0, φ_0, r, and T_e a solution of the system of equations (15)–(17) exists only in the region $0 \le z \le z_{cr}$. In the simulations, the quantity z_{cr} was identified with the depth of plasma penetration into the emission channel, L_{ch}.

Thus, the penetration of the plasma into the emission channel is accompanied by a decrease in its density and the appearance of an axial electric field, which returns electrons into the discharge gap. The decrease in plasma density results in a growth of the near-wall space charge layer, and this eventually may limit the plasma penetration depth. These factors substantially affect the characteristics of the electron emitter since, as the emission surface is displaced in the channel, for instance, under the action of the external electric field, the emission area and the density of the emitting plasma vary simultaneously.

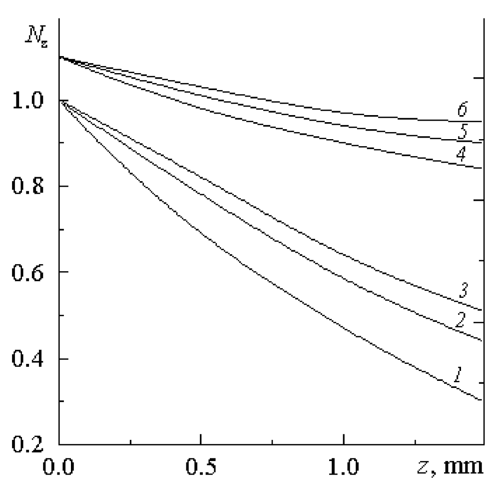

Fig. 4. The axial distributions of the plasma density (*1–3*) and potential (*4–6*) calculated for $R = 1$ (*1*, *4*), 2 (*2*, *5*), and 3 mm (*3*, *6*).

We estimate the effect of the electron emission on the parameters of the plasma in the intercathode space by using the system of equations (11) and (12). To do this, we add to Eq. (11) a term which takes into account the flux of electrons leaving the intercathode space in the direction of their emission (i.e., in the direction z):

$$\operatorname{div} j_e = (\beta + \gamma\beta)n + \alpha_n + \lambda - \frac{I_{em}}{e\pi R_e^2 L}. \quad (17)$$

Here, $I_{em} = \alpha I_d$ is the emission current, α is the emission efficiency, R_e is the radius of the surface from which electrons go away from the intercathode space. To simplify the calculations, we can assume $R_e = R$.

Figure 5 presents the radial distributions of the plasma density and potential calculated for different values of the emission current. If the electrons do not go away along the axis ($I_{em} = 0$), the limitation of their motion in the radial direction by the magnetic field results in highly nonuniform density and potential distributions (curves *1*). The appearing emission current reduces the plasma density and the radial gradient of plasma potential in the intercathode space of the discharge (curves *2*, *3*). As this takes place, the current of the electrons arriving at the anode decreases by the value of the emission current. This is due to the decrease in radial electron flux and in radial gradients of plasma density and potential with an increase in the flux of electrons going away along the discharge axis.

Analysis of the simulation results has shown that the degree of the influence of the electron emission on the density of the near-axis plasma may vary (Fig. 6). With a weak magnetic field and an elevated pressure in the discharge chamber, a mode is possible with negligible variations in plasma density during the extraction of electrons (curve *3*).

The electron emission, as well as affecting the plasma parameter, also leads to changes in discharge characteristics. An increase in emission current causes an increase in discharge operating voltage U_d. An increase in U_d is accompanied by an increase in cathode fall potential in the discharge and, hence, in ionizing power of γ-electrons, which is necessary to compensate the energetic electrons lost in emission.

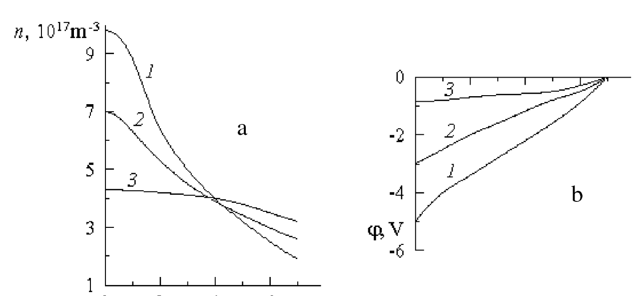

Fig. 5. The radial distributions of the plasma density (a) and potential (b) in a discharge ($I_d = 100$ mA) for the emission current $I_{em} = 0$ (*1*), 30 (*2*), and 50 mA (*3*).

https://doi.org/10.1017/S0263034603212027 Published online by Cambridge University Press

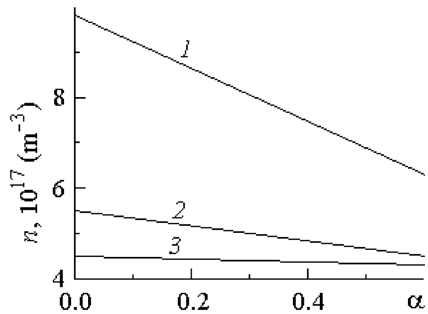

Fig. 6. Plasma density at the discharge axis versus emission efficiency for $p = 1$ (*1*) and 10 Pa (*2, 3*) and $B = 0.08$ (*1, 2*) and 0.05 T (*3*). Discharge current = 100 mA.

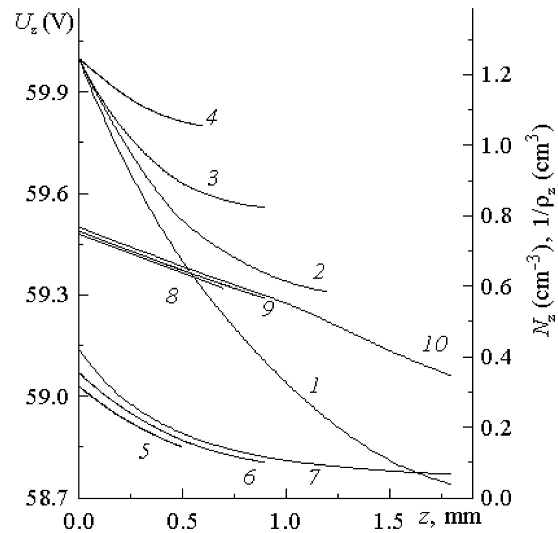

Fig. 7. The axial distributions of the plasma potential (*1–4*), density (*5–7*), and radius (*8–10*) for $n_0 = 10^{19}$ m^{-3}, $T_e = 5$ eV, $R = 1$ mm. Emission current $I_{em} = 0$ (*1, 7, 10*), 93 (*2*), 186 (*3, 6, 9*), and 372 mA (*4, 5, 8*).

The influence of the emission on the parameters of the plasma in the emission channel consists not only in varying the density n_0 at the channel inlet, but also in distorting the Boltzmann distribution of the electron density along the channel axis due to the appearance of the axial electron current. Moreover, since some electrons leave the plasma through the emitting surface, the fraction of electrons which return into the discharge from the channel decreases with increasing I_{em}, and the longitudinal field in the plasma penetrating into the channel weakens. These processes can be taken into account by complementing the right side of Eq. (16) with a term associated with the emission:

$$N_z = \exp(U_z - U_0) - \frac{I_{em}}{e\pi R^2 \rho_z^2 v_e(\xi)}. \qquad (18)$$

Here, $\xi = z/r_e$ and $v_e(\xi)$ is the average velocity of the emitted electrons in the cross section z. The quantity $v_e(\xi)$ is determined as

$$v_e(\xi) = \frac{\displaystyle\int_{v_e}^{\infty} \sqrt{v^2 - \frac{kT_e}{m_e}U_z}\sqrt{\frac{m_e}{\pi kT_e}}\, e^{-mv^2/kT_e} dv}{\displaystyle\int_{v_e}^{\infty} \sqrt{\frac{m_e}{\pi kT_e}}\, e^{-mv^2/kT_e} dv}, \qquad (19)$$

where $v_e = \sqrt{kT_e U_{em}/m_e}$ with $U_{em} = U(z)$ being the potential at the emitting boundary of the plasma.

Calculations show that for a constant n_0, the perturbation of the plasma in the channel during electron emission is reduced in the main to a decrease in its potential gradient with increasing I_{em} (Fig. 7). At the same time, the axial distributions of the plasma density and radius remain almost unchanged.

2.4. Emission characteristics of an electron emitter: Current control

By an emission characteristic of an electron emitter is meant a function of the emitter current on any parameter capable of changing this current. Such a parameter may be the gas pressure inside or outside the discharge, the magnetic field, the accelerating voltage, the discharge current, and so forth. It is important to know these functions, at least, for two reasons. First, the effect of some external factors, such as pressure, on the emission current may appear to be detrimental, and this will call for the development of an additional circuit for current stabilization. Second, of crucial importance for an emitter are the possibility and range of emission current control. Therefore, it is necessary to choose parameters by which the current could be controlled. In other words, some emission characteristics acquire the meaning of characteristics of emitter current control.

The effect of the gas pressure, the magnetic field, and some other factors have been considered above. Let us consider in more detail the dependence of the emission current on other parameters. For simplicity, in our general considerations we shall assume the density of the emitting plasma equal to the discharge plasma n_0.

Assuming that the velocity distribution of the plasma electrons is near-Maxwellian, we can represent the emission formula for an electron emitter as

$$I_{em} = 2\pi e (kT_e/2\pi m_e)^{1/2} \int_0^R n(r) e^{-e\varphi'(r)/kT_e} r\, dr, \qquad (20)$$

where $\varphi'(r)$ is the minimum potential in the emission region.

Depending on the proportion between the width of the near-wall layer, $l_{\text{КП}}$, and the radius of the emission hole, three typical situations, which have already been discussed, are possible.

1. The emitting plasma is separated from the electron acceleration region by a space where the potential is a minimum and electrons are braked by an electric field. The potential barrier in a plasma electron emitter, in contrast to a

https://doi.org/10.1017/S0263034603212027 Published online by Cambridge University Press

hot-cathode vacuum diode, cannot be created by a region of negative space charge. However, the potential minimum can be produced by the electric field of the emission electrode (Fig. 8a). In the type of emitter under consideration, electrons are extracted through the cathode hole. Hence, the total potential fall between the plasma and the emission electrode is an insuperable barrier to the plasma electrons, and the field of the acceleration electrode partially compensates the barrier in the region of cross-sectional area S_e. In this case, the emission formula (20) can be represented, for the region confined within the limits of S_e, in the form

$$I_{em} = e(kT_e/2\pi m_e)^{1/2} n_0 \pi (R - l_{cp})^2 e^{-e\varphi/kT_e}. \tag{21}$$

The emission current is formed by the electrons having overcome the potential barrier through the regions confined within the limits of S_e.

2. When the barrier is completely eliminated by the field of the collector or when the plasma parameters are such that the relation $l_{cp} < r$ is fulfilled even for the collector potential zero, electrons are emitted from an open plasma surface. A sketch of this type of emission system is shown in Figure 8b. For this case, the emission formula is

$$I_{em} = e(kT_e/2\pi m_e)^{1/2} n_0 \pi (R - l_{cp})^2 + e(kT_e/2\pi m_e)^{1/2} \int_{R-l_{cp}}^{r_e} n(r) e^{-e\varphi/kT_e}\, dr. \tag{22}$$

Neglecting, as above, the electron current through the near-wall ion layer, we may represent the emission formula in the form

$$I_{em} = e(kT_e/2\pi m_e)^{1/2} n_0 \pi (R - l_{cp})^2. \tag{23}$$

The emission area, and, hence, the emission current, strongly depend on the layer width l_{cp}.

3. If the condition $l_{\text{KП}} \ll r_э$ is fulfilled, the electron emission occurs, as in the second case, from an open plasma surface and the emission area depends in the main on the size of the emission hole. The emission formula takes the form

$$I_{em} = e(kT_e/2\pi m_e)^{1/2} n_0 \pi R^2.$$

In all the three situations above, the emission current is proportional to the plasma density n_0. It follows that, irrespective of the way by which the electron emission is realized—through a potential barrier or from an open plasma surface—the emission can be controlled by varying n_0. However, while this is the unique control method for the third case, in the situation illustrated by Figure 8b, the emission current can be controlled additionally by varying the potential barrier.

The control of the emitter current through variations in emitting plasma density is most frequently performed by varying the discharge current. This is realized in a rather simple way with a satisfactory characteristic slope. At the same time, this method has some limitations when using some types of discharge. Thus, with a hollow-cathode reflected discharge, this control has the following disadvantages:

1. Since a hollow-cathode discharge exists only with currents $I_d \geq I_{min}$, where I_{min} is the minimum current for a discharge to operate in a cavity, the beam current can be reduced only to $I_d = \alpha I_{min}$. The minimum beam current is generally 5–10 mA, which is inappropriate for some applications.
2. The possibilities for pulsed control of the emission are limited; this is related to the relatively long discharge formative time and the deionization of the discharge gap.
3. Some important emitter characteristics may vary with discharge current.

Thus, the maximum brightness B_{max} and power density g_{max} of focused electron beams produced by a plasma emitter, for a constant accelerating voltage U_{acc} of the electron source, as follows from the expressions

$$B_{max} = j_{em} \frac{eU_{acc}}{\pi k T_e \sin\theta}, \qquad g_{max} = j_{em} \frac{eU_{acc}}{kT_e} \sin^2\theta,$$

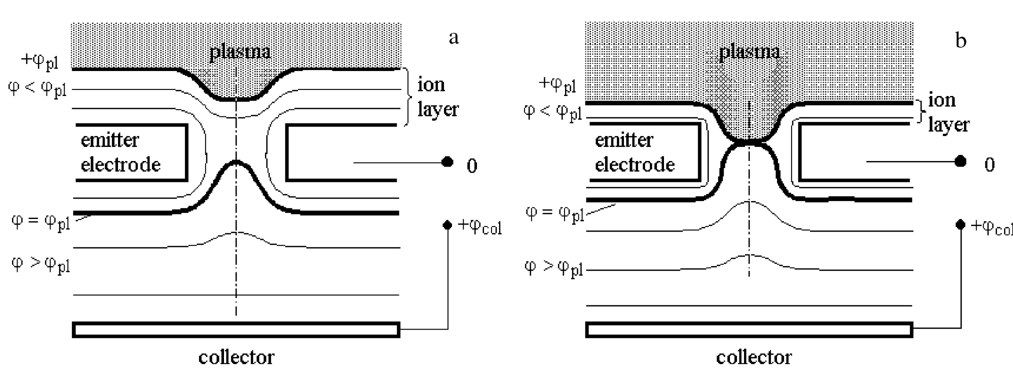

Fig. 8. Sketch of emission system with (a) and without (b) potential barier in emission range.

depend on the emission current density j_{em}. In the above expressions, θ is the half-angle of the beam convergence. Since the electron density in the emission region varies with current and, hence, so does j_{em}, high values of B_{max} and g_{max} generally cannot be attained at low emission currents.

From the viewpoint of the electron emission control, the emission from an open plasma surface whose dimensions are limited by a layer, that is, for $l \approx r$, is of greatest interest. Theoretically, in this case there exists a possibility to control the emission current by varying not only the discharge current, but also the emission area through the control of the ion layer width. Analysis and experiments have shown that for the type of discharge under consideration, the dimensions of the cathode layer can be varied by a relatively simple method, namely, by varying the potential of the emitter cathode relative to the second (hollow) cathode. In doing this, the discharge stability is not violated.

Let us calculate the control characteristics with due account for the processes occurring in the channel. To do this, we introduce into the formula for the emission current [formula (23)] the plasma density and the emitting surface radius as functions of z:

$$I_{em} = en(z_{em})v_e(z_{em})\pi r^2(z_{em}). \qquad (24)$$

z_{em} will depend on discharge current or accelerating voltage. Figure 9a presents calculated and experimental dependences $I_{em}(I_d)$. It can be seen that these dependences are nearly linear. Calculations show that the emission current increases with I_d as a result of increasing $n(z_{em})$ and $r(z_{em})$, and the position of the emitting boundary in this case varies insignificantly. For instance, for a channel with $r_{em} = 1$ mm at $U_{acc} = 20$ kV and I_d varied from 60 to 400 mA, I_{em} varies from 20 to 130 mA, and the displacement of the emitting surface is only 0.1 mm. Figure 9b gives calculated and experimental characteristics of the emission current controlled by varying the potential of a cathode with an emission hole, U_c. Calculations have shown that a variation in U_c varies not only the area of the emitting surface, but $n(z_{em})$ as well. The control characteristics calculated taking into account this factor agree with experimental results.

The dependence of the emission current on the accelerating voltage (current-voltage characteristic) is important in choosing the operating mode of the emitter in an electron source. Such a characteristic can be obtained taking into account the electric field distribution in the acceleration gap and the influence of this field on the position of the plasma boundary in the channel. Calculated and measured current-voltage characteristics of an emitter are given in Figure 10. These characteristics differ in discharge current. Herein, calculated dependences of the position z_{em} of the emitting plasma on the accelerating voltage are shown.

The increase in emission current with U_{acc} is due to the displacement of the emitting plasma boundary toward the inlet of the channel and the corresponding increase in emitting plasma density and in the area from which the emission occurs. As the discharge current is varied, the depth of penetration of the plasma into the channel varies as well; therefore, the mode of electron emission from an open plasma surface is realized starting from different values of U_{acc}. The bend in the characteristic and the tendency toward saturation are related, on the one hand, to the limited penetration of the field of the acceleration electrode into the emission channel and, on the other hand, to the screening of this field by the space charge of emitted electrons, which results from the increase in I_{em}.

2.5. Features of the pulse-controlled electron emission from plasma

In plasma electron sources, the processes of discharge initiation and plasma production have no effect upon the time parameters of the emission current pulse, since the source starts actively operating once the plasma has been produced. From the moment of discharge initiation, when the source is only under the negative bias voltage U_{bias}, which prevents electrons from penetration into the acceleration gap, the source is idling. Once the plasma production has been completed, a positive pulsed voltage is applied to the grid from a nanosecond pulse generator. This results in a stepwise increase in the potential of the control grid rela-

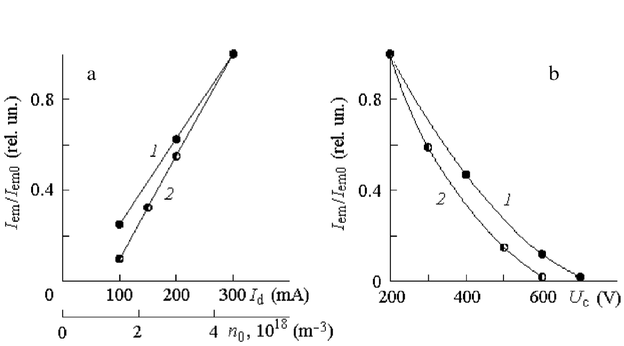

Fig. 9. The dependence of the emission current on plasma density and discharge current (a) for $U_{acc} = 25$ (*1*) and 5 kV (*2*) and on cathode potential (b) at $U_{acc} = 25$ kV, $n_0 = 5\cdot10^{18}$ (*1*) and $3\cdot10^{18}$ m^{-3} (*2*).

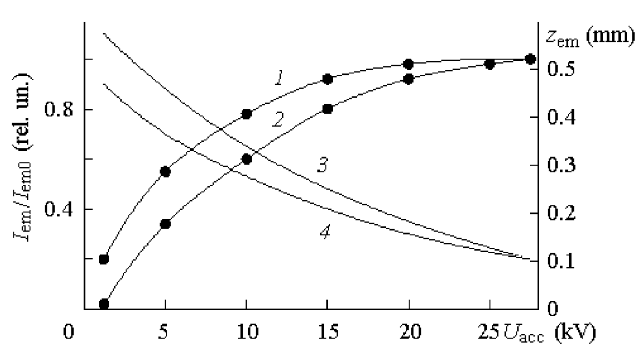

Fig. 10. The dependences of the emission current (*1*, *2*) and of the position of the plasma emitting boundary (*3*, *4*) on accelerating voltage. Lines: calculation, dots: experiment.

https://doi.org/10.1017/S0263034603212027 Published online by Cambridge University Press

tive to the anode, in a redistribution of the current between the anode and the control grid, and in changes in the heights of the potential barriers and in the widths of the near-electrode layers. To simplify the analysis of the plasma processes, we shall assume that the plasma is confined in between two plane electrodes: the anode and the grid. At the time zero (t_0), the applied potential difference is uniformly distributed over the width of the electrode gap. The motion of electrons toward the control grid has the result that the near-anode space charge layer expands. As this layer expands, the fall voltage across the layer increases, while the field strength in the plasma decreases. At some point in time, the field in the plasma is compensated by the space charge field of the anode layer. The electrons go on moving, giving rise to a field of reverse polarity in the plasma, which brakes electrons and again reverses the direction of their motion. Oscillations of the electron cloud appear in the plasma (Singh Nagendra, 1982). These oscillations are damped out within the time (Alekseev *et al*., 1979)

$$t_1 = 0.2\left(\frac{m_i}{8\pi n_i e^2}\right). \tag{25}$$

Under the conditions of an experiment with $m_i = 2.18 \cdot 10^{-22}$ g (for Xe) and $n_i = 5 \cdot 10^{11}$ cm^{-3}, the damping time t_1 is of the order of 10^{-9} s. Under actual experimental conditions, the duration of this process is considerably shorter than the rise time of the voltage across the control grid; therefore, the electrons have time to attain local equilibrium within a time of the order of or less than the characteristic potential variation time. As a result, there is no amplitude modulation of the electron current due to the oscillations of the electron cloud.

The new potential barrier for the electrons going away toward the anode and the invariable height of the potential barrier near the grid are responsible for the decrease in the total number of electrons leaving the plasma. If the cathode (discharge) current is a constant, an additional negative charge is accumulated in the plasma that reduces the plasma potential relative to the electrodes. This, in turn, increases the electron current from the plasma, mainly, the current onto the grid. The process ends in the recovery of the continuity of the conduction current in the plasma.

For electron emission from plasma occurring through a potential barrier, the establishment of current can be described by the equation (Galansky *et al*., 1988)

$$eV\frac{d(\langle\Delta n_e\rangle)}{dt} = I_d - j_{ch}S_a \exp\left[-\frac{e(\varphi + U_0)}{kT_e}\right] - j_{ch}S_g \exp\left(-\frac{e\varphi}{kT_e}\right), \tag{26}$$

where V is the volume of the electron gap, $\langle\Delta n_e\rangle$ is the volume-averaged excessive electron density in the plasma, I_d is the discharge current, j_{ch} is the chaotic electron current density in the plasma, and φ is the potential of the plasma.

Under the assumption that $\varphi = \varphi_0 - A\langle\Delta n_e\rangle$, where $A =$ const, and in view of the fact that under actual condi-tions $\langle\Delta n_e\rangle \ll n_e$ (Martens, 1986), the solution of Eq. (26) gives us

$$\frac{I_c}{I_{c0}} = \frac{\alpha \exp(t/\tau)}{\alpha - 1 + \exp(t/\tau)}, \tag{27}$$

where $I_c = j_{ch}S_g \exp(-e\varphi/kT_e)$, $I_{c0} = j_{ch}S_g \exp(-e\varphi_0/kT_e)$, $\alpha = (S_a + S_g)/[S_a \exp(eU_0/kT_e) + S_g]$ is a factor which characterizes the degree of rise of the grid current, $\tau = kT_e/(AI_d)$ is the time constant for current establishment, V is the volume of the discharge system, and T_e is the electron temperature.

The calculation of τ for typical experimental conditions (Gushenets *et al.*, 1990) gives a value close in order of magnitude to 10^{-9} s. The transient process of current establishment is complete in a time $t = (3–5)\tau$. In analyzing the processes of current switching, the motion of ions was not taken into account and it was assumed that, in view of the great difference in masses between electrons and ions, the latter are immobile. Under typical experimental conditions, the plasma has a positive potential relative to the hollow anode and the more so as relative to the negatively biased grid. Therefore, a positive space charge layer appears near the walls of these electrodes. As mentioned above, a variation in grid voltage varies the plasma potential and, hence, the width of the space charge layer. Since ions prevail in this layer, it can be supposed that it is the motion of ions that determines the dynamics of the layer. To describe the motion of the layer boundary, we use a continuity equation for an ion current (Varey & Sander, 1969):

$$j(t) = en_0(u_0 + dl_s/dt). \tag{28}$$

Here, enu_0 is the ion current from plasma (Bohm's current) and $en_0(dl_s/dt)$ is the ion current component in the frame of reference related to the moving layer. The current in the layer is determined by the "3/2-power law." As a result, we get the following equation:

$$\frac{1}{9\pi}\left(\frac{e}{M_i}\right)^{1/2}\frac{\Delta\varphi^{3/2}}{l_s^2(t)} = 0.4en_0\left(\frac{2kT_e}{M_i}\right)^{1/2} + en_0\frac{dl_s(t)}{dt}. \tag{29}$$

Introducing dimensionless variables, we get a solution of Eq. (29) in the form

$$\tau = 1.77\left[(\xi_0 - \xi) + \frac{\psi}{2}\ln\left(\frac{\psi + \xi\psi - \xi_0}{\psi - \xi\psi + \xi_0}\right)\right]. \tag{30}$$

The establishment of the positive space charge layer of width l_s is a rather prolonged process. For the plasma parameters close to those realized in experiment, relation (30) predicts that the process is complete within a time longer than 10^{-7} s.

Thus, if the rise time of the pulsed control voltage is longer than a few nanoseconds, two modes of electron extraction from the plasma are realizable. These modes differ by the degree of influence of the process of establishment of the position of the layer boundary upon the amplitude and waveform of the pulsed emission current. For the first mode, where the width of the space charge layer near the control grid is much greater than the size of the grid mesh at any point in time, the emission current rise rate is determined only by the lowering of the height of the potential barrier resulting from the change in excessive charge in the plasma, $\langle \Delta n_e \rangle$. In this case, it is possible to produce an electron beam with the current rise time shorter than 10 ns, the waveform having an almost flat top, and the amplitude proportional to the transmittance of the grid. For the second mode, as the layer boundary is displaced, the layer width becomes less than the size of the grid mesh, and the height of the potential barrier to electrons varies not only due to the decrease in $\langle \Delta n_e \rangle$, but also due to the fact that the collector field penetrates through the emission grid meshes. In this case, the beam current pulse has two sections with different rise rates. For the first section, the current rise rate depends on the charge variation rate $\langle \Delta n_e \rangle$, while for the second one it is determined by the velocity of motion of the boundary of the space charge layer.

3. EMISSION METHODS FOR STUDYING FUNDAMENTAL PROCESSES IN THE PLASMA OF A VACUUM ARC DISCHARGE

The emission methods for studying the processes occurring in a vacuum arc discharge that we currently develop involve the determination of the parameters and characteristics of the discharge plasma by analyzing the ion current extracted from the plasma and the charge components of this current. The principal methodical difficulties arising in studying the plasma of a vacuum arc are associated with the fact that the cathode spot is small in size ($<10^{-2}$ cm), takes a random position, and moves with a velocity of $\sim 10^4$ cm/s over the cathode surface, and the plasma density in the region adjacent to the cathode spot is $>10^{16}$ cm^{-3}. These features of the cathode spot as a physical object plague its experimental investigation. In view of this, corpuscular diagnostic methods, such as the emission method (Bugaev *et al.*, 2000*a*; Yushkov *et al.*, 2001), seem to be, perhaps, the only approach that can be used to study the cathode spot phenomena experimentally. The essence of the method is to investigate the reaction of the charge distribution of the ions extracted from the emission boundary located far away from the cathode spots of the vacuum arc to the action experienced by the discharge. This action may be an abrupt change in vacuum arc current, which results in the death of the existing cathode spots or in the birth of new ones.

The electrode assembly of the experimental setup is shown schematically in Figure 11. The vacuum arc discharge was initiated in the discharge gap formed by cathode *1* and

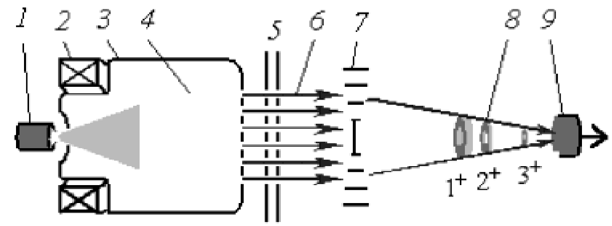

Fig. 11. Electrode assembly of a setup for investigations of the ion velocity: *1*: cathode, *2*: solenoid, *3*: anode, *4*: vacuum arc plasma flow, *5*: accelerating electrodes, *6*: ion beam, *7*: spectrometer gate, *8*: ions of different charge, *9*: Faraday cup.

anode *3*. The discharge current pulse width and current were, respectively, 200–500 μs and 100–500 A. During the operation of the arc, plasma *4* of the cathode material filled the cavity of electrode *3*. The end face of anode *3* had emission holes for the extraction of ions from the plasma. The extracted ions were accelerated in multiaperture acceleration–deceleration system *5* by a dc voltage of 10–30 kV. The charge state of ion flow *6* was analyzed with the use of a time-of-flight mass spectrometer (Brown *et al.*, 1987; Bugaev *et al.*, 2000*b*).

After >150 μs from the initiation of the vacuum arc, when all its principal parameters could be considered steady, an additional current pulse was applied to the discharge gap or the power supply of the discharge was closed with a fast switch (Yushkov, 2000). In the first case, the arc current increased by 50–150 A within 2–4 μs, while in the second one, it decreased to zero within about 2 μs, leading to extinction of the discharge (Fig. 12). Below, when describing the mentioned variations in arc current, we shall use the terms "current step" and "current cutoff."

Noteworthy is the fact that both when the current of a vacuum arc discharge experienced a jump and when its cutoff took place, the reaction of the ion beam current to the mentioned perturbations of the arc current was observed after a time t_{ib}.

The time t_{ib} fixed in experiment depends on the cathode material and equals 8 μs for the lightest material (C) and 40 μs (Bi). At the same time, the time it took for ions of these elements to pass through the acceleration gap and the drift space was, respectively, less than 1 and 3 μs. Obviously, this substantial excess in t_{ib} is due to the motion of ions in the plasma from the cathode region, where they are generated, to the emission grid. By the changes in currents of each ion species it could be determined in which time after the action experienced by the vacuum arc the emission current extracted from the discharge plasma changed and thus the velocity of motion of the ions from the vacuum arc cathode spot to the emission surface could be estimated.

Typical dependences of the currents of different ion species on the time lapsed after the application of an additional current step to the discharge gap are given in Figure 13 for a vacuum arc with a magnesium cathode. Herein, the respective dependences for the case of an arc current cutoff are

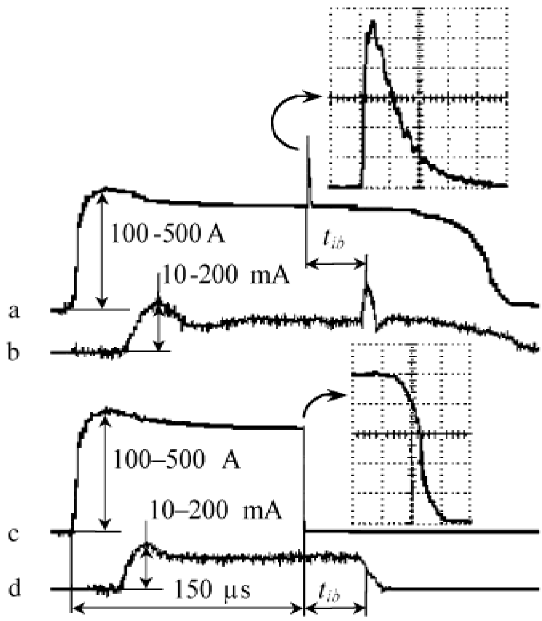

Fig. 12. Waveforms of the vacuum arc current (a, c) and ion beam current (b, d) for a "step" (a, b) and a "cutoff" (c, d) of the arc current. The arc current waveforms recorded at the instant of the respective "current step" or "current cutoff" are given in the insets. 1 μs/div, 25 A/div.

shown. It should be noted that when a current step is applied to the discharge gap, the currents of different ion species peak at the same time, and when the discharge current is cut off, the currents of different ion species fall in the same fashion. The above behavior was observed for all cathode materials tested, namely, for Mg, Al, Ti, Zr, Cu, Pb, and Bi.

For both a vacuum arc current step and a current cutoff, the reaction of the ion current shows up after a time t. Since the ionization of the cathode material in a vacuum arc occurs in the main near the cathode spots at distances not over 1 mm from the cathode surface, which is much less than the

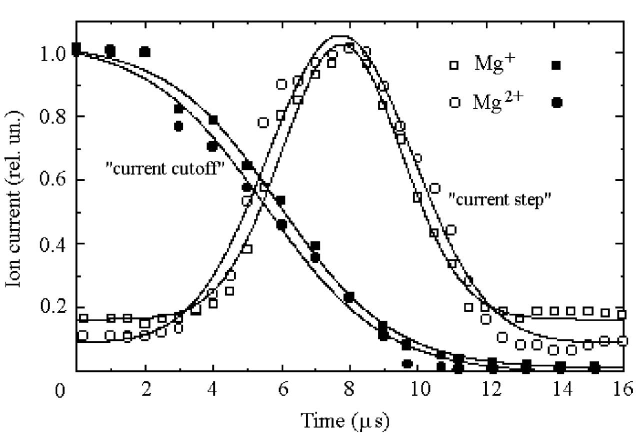

Fig. 13. Evolution of the currents of different ion species after the application of a current "step" to the discharge gap and after a "cutoff" of the current of a vacuum arc discharge. Cathode material: Mg.

distance $L_{\kappa a}$, and later only adiabatic expansion of the plasma flare takes place (Mesyats, 1994), the velocity of the plasma ions, v_i, can be determined as

$$v_i = \frac{L_{c\text{-}a}}{t - (L_з + 2d_{acc})\sqrt{M_i/2QeU_{acc}}}, \tag{31}$$

where U_{acc} is the accelerating voltage; M_i and Qe are the ion mass and charge, respectively; d_{acc} is the acceleration gap spacing; and $L_з$ is the distance from the acceleration electrode to the gate of the mass spectrometer. For the case of a current step, the value of t was determined as the time interval between the points where the discharge and the ion current peaked, while for the case of a current cutoff, the value of t was taken as the time interval between the maxima of the time-differentiable waveforms of these currents. The investigations performed have shown that differently charged ions of the same material have almost the same velocities of directional motion. Differentiating the ion current waveform with respect to time, one can obtain a directional velocity distribution function for ions, the distributions for different ion species practically coinciding.

Since it had been established exactly that the directional velocities of differently charged ions are in fact the same for $p < 5 \cdot 10^{-5}$ Torr, there was no need to use the time-of-flight spectrometer, which was intended to separate the ion component of the plasma into differently charged fractions, in further investigations of the directional velocities of ions. These experiments featured a slower modulation of the arc current pulse with the characteristic oscillation time $\tau \approx$ 50 μm and the amplitude making up not over 30% of the pulse current and the use of a single plain Langmuir probe to record the ion component of the plasma. The velocity of ions in these experiments was estimated as $v_i = L_{c\text{-}pr}/\Delta t$, where Δt is the time lag between the oscillations of the discharge and probe currents (Fig. 14) and $L_{c\text{-}pr}$ is the distance between the cathode and the probe surface. The measured velocities of ions for different cathode materials, including most of the conducting materials of the periodic table of elements, and the vacuum arc operating voltages are given in Table 1.

A two-fluid hydrodynamic model of the plasma of a cathode flare, which consists of electrons and ions with an average charge number $\langle Q \rangle$, adiabatically expanding after the explosive formation of an "ecton," has been developed by Mesyats *et al.* (Litvinov, 1974; Bugaev *et al.*, 1975; Mesyats & Proskurovsky, 1986; Mesyats, 1994). According to the results of these investigations (Mesyats & Proskurovsky, 1986), the velocity of expansion of a cathode flare at a large distance from the cathode spot, which is equal to the directional velocity of the ions, v_i, can be determined as

$$v_i = \frac{2}{\gamma - 1}\sqrt{\frac{\gamma(\langle Q \rangle T_e + T_i)}{M_i}}, \tag{32}$$

https://doi.org/10.1017/S0263034603212027 Published online by Cambridge University Press

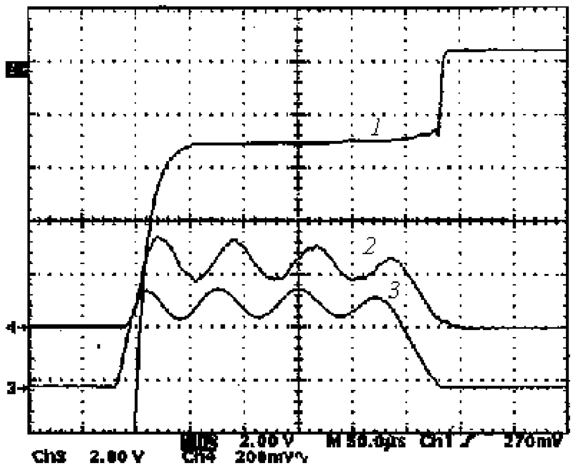

Fig. 14. Waveforms of the operating voltage (*1*), probe ion current (*2*), and discharge current (*3*) for a vacuum arc with a Ta-cathode: *1*: 20 V/div; *2*: 0.1 A/div; *3*: 200 A/div. The distance from the cathode to the probe is 24 cm. The time lag between the oscillations of the discharge and probe currents is 20 μs and corresponds to the Ta ion velocity $v_i = 1.2 \cdot 10^6$ cm/s.

where γ is the adiabatic exponent equal to 5/3. Assuming, as in Mesyats and Proskurovsky (1986) that $T_e \approx T_i$, and substituting the numerical values of $\langle Q \rangle$ and T_e from Table 1, we can estimate the directional velocities of the ions. The results of this estimation are compared with experimental data in Figure 15. The high degree of agreement between estimates and measurements allows the conclusion that the hydrodynamic mechanism dominates in the achievement by ions of the observed velocities, and expression (32) by itself accounts for the dependence of v_i on $\langle Q \rangle$ and M_i and, as $T_e \propto U_d$, on U_d, observed in experiment. The hydrodynamic model of the acceleration of ions in the cathode region of a vacuum arc (Yushkov *et al.*, 2001), which was proposed to describe the results of the investigations under consideration, is based on the idea that the cathode material is additionally accelerated after its transition to the state of completely ionized collisional plasma. As in the model described in Litvinov (1974), Bugaev *et al.* (1975), and Mesyats and Proskurovsky (1986), the reason for this acceleration is the expansion of the plasma into vacuum under the condition that there is continuous energy delivery due to Joule heating. By way of comparing simulation predictions with measurements, it has been shown that the cathode material is accelerated predominantly, when it is in the state of a completely ionized ideal plasma, through its hydrodynamic expansion into vacuum and the ion velocities at a considerable distance from the vacuum arc cathode spot are given by

$$v_i = 3.5\sqrt{\gamma \langle Q \rangle T_e / M_i}. \tag{33}$$

Calculated values of ion velocities are also given in Figure 15. Good correlation with measurements and predictions based on expression (32) is observed. An important feature of these investigations is the opportunity to calculate

Table 1.

Element	Atomic number	v_i,10^6 (cm/s)	U_d, V	$\langle Q \rangle$	T_e, eV
Li	3	2.3	23.5	1	2
C	6	1.7	31	1	2
Mg	12	2	18.6	1.5	2.1
Al	13	1.5	22.6	1.7	3.1
Si	14	1.5	21	1.4	2
Ca	20	1.4	20.5	1.9	2.2
Sc	21	1.5	21.6	1.8	2.4
Ti	22	1.5	22.1	2	3.2
V	23	1.6	22.7	2.1	3.4
Cr	24	1.6	22.7	2.1	3.4
Fe	26	1.3	21.7	1.8	3.4
Co	27	1.2	21.8	1.7	3
Ni	28	1.2	21.7	1.8	3
Cu	29	1.3	22.7	2	3.5
Zn	30	1	17.1	1.2	2
Ge	32	1.1	20	1.4	2
Sr	38	1.2	18.5	2	2.5
Y	39	1.3	19.9	2.3	2.4
Zr	40	1.5	22.7	2.6	3.7
Nb	41	1.6	27.9	3	4
Mo	42	1.7	29.5	3.1	4.5
Rh	45	1.5	23.8	1.8	4.5
Pd	46	1.2	23.5	1.9	3.5
Ag	47	1.1	22.8	2.1	4
Cd	48	0.7	14.7	1.3	2.1
In	49	0.6	16	1.3	2.1
Sn	50	0.7	17.4	1.5	2.1
Ba	56	0.8	16.5	2	2.3
La	57	0.7	18.7	2.2	1.4
Ce	58	0.8	17.6	2.1	1.7
Pr	59	0.8	20.5	2.3	2.5
Nd	60	0.8	19.2	2.2	1.6
Sm	62	0.8	18.8	2.1	2.2
Gd	64	0.8	20.4	2.2	1.7
Tb	65	0.8	19.6	2.2	2.1
Dy	66	0.8	19.8	2.3	2.4
Ho	67	0.9	20	2.3	2.4
Er	68	0.9	19.2	2.3	2
Hf	72	1	23.3	2.9	3.6
Ta	73	1.2	28.6	2.9	3.7
W	74	1.1	28.7	3.1	4.3
Ir	77	1.1	25.5	2.7	4.2
Pt	78	0.8	23.7	2.1	4
Au	79	0.7	19.7	2	4
Pb	82	0.6	17.3	1.6	2
Bi	83	0.5	14.4	1.2	1.8
Th	90	1.0	23.3	2.9	2.4
U	92	1.1	23.5	2.3	3.4

directional velocities of variously charged ions. Simulations have predicted that the velocities of variously charged ions can be different from their common hydrodynamic velocity only by a few percent, and this agrees with the experimental data obtained.

In conclusion, it should be noted that, according to the hydrodynamic models considered, the factors dominating the value of the directional velocity of ions should be the mass of the ions, their average charge, and the electron

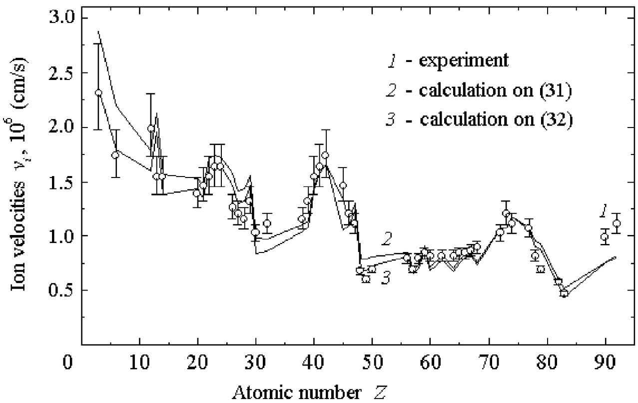

Fig. 15. The directed velocities of the vacuum arc plasma ions measured (*1*) and calculated based on hydrodynamical models (*2,3*) for various cathode materials.

temperature, and this is in complete agreement with the experimental results obtained.

The experimental investigations of the directional velocities of ions make it possible to uniquely relate the density of the saturation ion current onto a plane Langmuir probe placed normal to the plasma flow and with the parameters of the plasma:

$$j_i = e\langle Q\rangle n v_i = e\langle Q\rangle n(20T_e\langle Q\rangle M_i)^{1/2}. \tag{34}$$

The use of expression (34) is more justifiable than the frequently used Bohm formula (Alekseev & Kotel'nikov, 1988; see, e.g., Brown, 1989, p. 344), which was deduced on the assumption that the ions of a vacuum arc move with the sound velocity. At the same time, the experimental result obtained show that the directional velocities of ions are substantially greater than ion sound velocities. It can readily be shown that the Bohm formula, when used to determine the plasma density by the ion current onto a plane probe, gives a more than threefold underestimated value. The comprehensive measurements of the directed velocities of the ions of the plasma of a vacuum arc discharge, performed for most of the metals of the periodic table, not only are of practical importance, but also have a decisive significance for the understanding of the physical nature of cathode spots.

ACKNOWLEDGMENTS

Research contracts with Lawrence Berkeley and Brookhaven National Laboratories, USA, IPP Trust-I American-Russian scientific cooperation program, CRDF grants GAP # REO-10202-BNL, GAP # REO-10614-LBNL, and BRHE # TO-016-02 are gratefully acknowledged.

REFERENCES

Alekseev, B.V. & Kotel'nikov, V.A. (1988). *The Probe Method for Plasma Diagnostics*. Moscow: Energoatomizdat (in Russian).

Alekseev, B.V., Kotel'nikov, V.A. & Novikov, V.N. (1979). Calculation of disturbed layer around probe by numerical method. *Fizika Plazmy* **5**, 920–922.

Brown, I.G., Galvin, J.E., MacGill, R.A. & Wright, R.T. (1987). Improved time-of-flight ion charge state diagnostic. *Rev. Sci. Instrum.* **58**, 1589–1592.

Brown, I.G. (Ed.). (1989). *The Physics and Technology of Ion Sources*. New York: Wiley.

Bugaev, A.S., Gushenets, V.I., Nikolaev, A.G., Oks, E.M. & Yushkov, G.Yu. (2000*a*). Study of directed ion velocities in a vacuum arc by an emission method. *Zh. Tekhn. Fiz.* **70**, 37–43.

Bugaev, A.S., Gushenets, V.I., Nikolaev, A.G., Oks, E.M. & Yushkov, G.Yu. (2000*b*). Investigation "Titan" ion source by time-of-flight spectrometer. *Izv. Vyssh. Uchebn. Zaved.: Fizika*. No. 2, 21–28.

Bugaev, A.S., Vizir, A.V., Gushenets, V.I., Nikolaev, A.G., Oks, E.M., Yushkov, G.Yu., Burachevsky, Yu.A., Burdovitsyn, V.A., Osipov, I.V. & Rempe, N.G. (2003). Current status of plasma emission electronics: II. Hardware. *Laser Part. Beams* **21**.

Bugaev, S.P., Litvinov, E.A., Mesyats, G.A. & Proskurovsky, D.I. (1975). Electron explosive emission. *Usp. Fiz. Nauk* **115**, 102–120.

Bugaev, S.P., Kreindel, Yu.E. & Schanin, P.M. (1980). *Broad Beam Electron Sources*. Moscow: Energoatomizdat. (in Russian)

Galansky, V.L., Gruzdev, V.A., Zelensky, V.I., Osipov, I.V. & Rempe, N.G. (1990). Plasma characteristics in emission channel of plasma emitter. *Zh. Tekhn. Fiz.* **60**, 168–170.

Galansky, V.L., Gushenets, V.I. & Oks, E.M. (1988). Analysis of grid control of plasma cathode. *Abstracts of Seven All-Union Symp. on High-Current Electronics*. Vol. 1, pp. 89–91. Tomsk, USSR: High Current Electronics Institute.

Gavrilov, N.V. & Oks, E.M. (2000). High-current pulse sources of broad beams of gas and metal ions for surface treatment. *Nucl. Instrum. Meth. Phys. Res. A* **439**, 31–44.

Goebel, D.M. & Watkings, R.M. (2000). High current, low pressure plasma cathode electron gun. *Rev. Sci. Instrum.* **71**, 388–398.

Gruzdev, V.A. & Rempe, N.G. (1982). Peculiarities of current control in high intensive electron emitter. *Izv. AN SSSR. Ser. fiz.* **46**, 1324–1327.

Gushenets, V.I., Koval, N.N. & Schanin, P.M. (1990). Generation of nanosecond high-current electron beams with a high pulse repetition rate. *Pis'ma Zh. Tekhn. Fiz.* **16**, 12–16.

Hershcovitch, A., Johnson, B.M., Liu, F., Anders, A., & Brown, I.G. (1998). Results from energetic electron beam metal vapor vacuum arc and Z-discharge plasma metal vapor vacuum arc: Development of new sources of intense high charge state heavy-ion beams. *Rev. Sci. Instrum.* **69**, 798–800.

Koval, N.N., Oks, E.M., Schanin, P.M., Kreindel, Yu.E. & Gavrilov, N.V. (1992). Broad beam electron sources with plasma cathodes. *Nucl. Instrum. Methods Phys. Res. A* **321**, 417–428.

Kreindel, Yu.E. (1977). *Plasma Electron Sources*. Moscow: Atomizdat (in Russian).

Kreindel, Yu.E. (Ed.). (1983). *Electron Sources with Plasma Emitter*. Novosibirsk: Nauka (in Russian).

Litvinov, E.A. (1974). In *Power Pulsed Sources of Accelerated Electrons*. pp. 23–34. Novosibirsk: Nauka (in Russian).

Martens, V.Ya. (1986). About ability of realization of positively charged electron beam. *Pis'ma Zh. Tekhn. Fiz.* **12**, 769–771.

https://doi.org/10.1017/S0263034603212027 Published online by Cambridge University Press

Mesyats, G.A. & Proskurovsky, D.I. (1986). *Pulsed Electrical Discharge in Vacuum*. Berlin-Heidelberg: Springer-Verlag.

Mesyats, G.A. (1994). *Ectons in a Vacuum Arc Discharge: The Breakdown, the Spark, and the Arc*. Ekaterinburg: Nauka (in Russian).

Oks, E.M. & Schanin, P.M. (1999). Development of plasma cathode elctron. *Physics of Plasmas* **6**, 1649–1654.

Schanin, P.M. (Ed.). (1993). *Charged-Particle Beam Sources with a Plasma Emitter*. Ekaterinburg: Nauka (in Russian).

Singh Nagendra (1982). Double layer formation. *Plasma Phys.* **24**, 639–660.

Varey, R.H. & Sander, K.F. (1969). Dynamic sheath growth in mercury plasma. *Brit. J. Appl. Phys. (J. Phys. D) Ser. 2*. **2**, 541–550.

Wolf, B.H. (Ed.). (1995). *Handbook of Ion Sources*. Boca Ration, FL: CRC Press.

Yushkov, G. (2000). Measurement of directed ion velocity in vacuum arc plasmas by arc current perturbation methods. *Proc. XIX Int. Symp. on Discharges and Electrical Insulation in Vacuum*, vol. I, pp. 260–263. China: Xi'an.

Yushkov, G.Yu., Bugaev, A.S., Krinberg, I.A. & Oks, E.M. . (2001). About mechanism of ion acceleration in vacuum arc plasma. *Dokl. RAN* **238**, 41–43.

Zarinov, A.V., Kovalenko, Yu.A., Roganov, I.S. & Tyuryukanov, P.M. (1986). Plasma cathode electron gun with grid stabilization. *Zh. Tekhn. Fiz.* **56**, 687–691.

Zavialov, M.A. *et al*. (1988). *Plasma Processes in Technological Electron Guns*. Energoatomizdat, Moscow (in Russian).